Journal of Colloid and Interface Science 462 (2016) 19–28

Contents lists available at ScienceDirect

Journal of Colloid and Interface Science

journal homepage: www.elsevier.com/locate/jcis

Enhancement of Localized Surface Plasmon Resonance polymer based biosensor chips using well-defined glycopolymers for lectin detection

Yan Jin, Kok Hou Wong, Anthony Michael Granville *

Centre for Advanced Macromolecular Design, School of Chemical Engineering, University of New South Wales, Sydney, Australia

HIGHLIGHTS

- A polymer based LSPR biosensor chip was fabricated for the detection of con A.
- Glycopolymers, with different M_n, were synthesized *via* a RAFT and "click" reactions.
- Glycopolymer clusters dramatically expanded sensors response to over 1 μmol L^{-1}.
- 10–16 glucose glycopolymer achieved balanced performance for sensitivity and response.

GRAPHICAL ABSTRACT

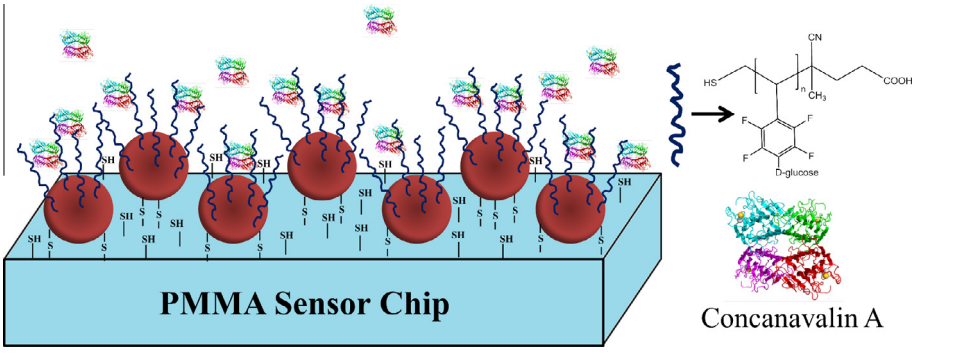

ARTICLE INFO

Article history:
Received 13 August 2015
Revised 17 September 2015
Accepted 20 September 2015
Available online 21 September 2015

Keywords:
Localized Surface Plasmon Resonance
Poly(pentafluorostyrene)
Reversible addition–fragmentation chain transfer
Glycocluster effect
Biosensor chips

ABSTRACT

Poly(methyl methacrylate) polymer based Localized Surface Plasmon Resonance biosensor chips were successfully fabricated using glycopolymer brushes carrying glucose moieties for the detection of concanavalin A. Poly(pentafluorostyrene), with pre-determined polymer chain lengths, were synthesized *via* a reversible addition–fragmentation chain transfer polymerization technique. The synthesized poly (pentafluorostyrene), was subsequently converted into glycopolymers *via* a *para*-fluoro-thiol "click" reaction and grafted onto the surface of sensor chips. The "glycocluster effect" induced by pendent carbohydrate moieties enabled a stronger affinity for concanavalin A binding, which resulted in a dramatic expansion of the sensors' response range. It was discovered that the longer polymer brushes did not guarantee additional enhancements for the sensor chips. Instead, they could lead to higher detection limits. In this study, the limit of detection for the sensor chips was discovered to be 1.3 nmol L^{-1} with a saturated response at 1054.2 nmol L^{-1}. In addition to the superior performance, the capabilities of the reported sensor chips can be easily manipulated to detect a diverse range of analytes by "clicking" various sensing elements onto the polymer brushes.

1. Introduction

Localized Surface Plasmon Resonance (LSPR) optical biosensors have drawn considerable interest in recent years due to their real-time, label-free biomolecule detection capabilities with ultra-high sensitivity [1]. Label-free sensing of an LSPR optical biosensor is usually achieved *via* functionalization of a sensor surface with moieties that can trigger variations in the surface refractive index through either adsorption of, or reaction with, analytes [2]. Among the metal particles used in LSPR sensing, gold nanoparticles (AuNPs) are the most preferred candidate due to

* Corresponding author.
E-mail address: a.granville@unsw.edu.au (A.M. Granville).

http://dx.doi.org/10.1016/j.jcis.2015.09.047
0021-9797/

their stability and biocompatibility [3]. For the detection of lectins, one of the frequently adopted strategies is the decoration of surface immobilized AuNPs with carbohydrates. However, several crucial factors need to be brought into consideration when designing an LSPR biosensor for lectin detection. Firstly, due to the rather large nature of the target lectins, steric hindrance due to analyte binding and crowding on the sensor surface is highly prevalent [4]. Additionally, the sensing carbohydrates generally only bind with specific sites on the lectin that often are located at the lectin interior, leading to hidden or inaccessible binding sites [5]. Finally, the interactions between a lectin and a carbohydrate molecule are usually weak, with dissociation constants typically in the millimolar range, several orders higher than that of antigen–antibody interactions [6].

To address some of these issues, poly(ethylene glycol) (PEG) has been employed in previous designs as the linker between AuNPs and carbohydrates [7,8]. Carbohydrate moieties were first incorporated onto the terminus of PEG chains which were subsequently anchored onto the AuNPs through Au–S covalent bonds at the other chain end. PEG on the AuNPs provides carbohydrate moieties with higher flexibilities and was shown to reduce the hindrance effect for lectin bindings. Recently, 1-dodecanethiol (DDT) was used to decorate AuNP surfaces, allowing physical entrapment of glycolipids [4]. The application of a DDT layer increased the space between the particle surface and carbohydrate moieties, resulting in better lectin binding. Based on this similar mechanism, poly (amidoamine) (PAMAM) dendrimers were successfully employed as the intermediate layer for the reduction of lectin binding hindrance [9]. However, the aforementioned techniques only considered the first two factors in the sensor design, the binding strength between lectin and carbohydrate remains mostly unchanged, and hence there is still a great potential to improve sensor performance. Glycopolymers, a type of polymeric material bearing pendant carbohydrates, have recently attracted interest in the field of drug delivery, cell culture substrates and surface modifications [10,11]. Glycopolymers can induce strong interactions with lectins by the multivalent effect of densely packed carbohydrates on the polymer chains, termed the "glycocluster effect" [12]. Utilizing glycopolymers in the fabrication of LSPR optical sensors for lectin detection could meet all three criteria listed previously: the polymer chains provide carbohydrates with increased flexibilities as well as extra space from the substrate surface to reduce the steric hindrance, while the closely packed carbohydrates will induce the "glycocluster effect" to enhance the interactions with the target lectins.

Synthesis of well-defined glycopolymers is always a demanding process because it requires mild reaction conditions to prevent degradation. Glycopolymers can be synthesized *via* two methods: the polymerization of sugar monomers or post modification of a preformed polymer by using active sugar substrates. So far, the synthesis of glycopolymers from sugar monomers remains difficult. It involves multiple preparation steps as well as demanding purification procedures [13,14]. In contrast, post-modification of polymers to yield functional glycopolymers is far less challenging. Over the years, there are several advancements which have been reported on the synthesis of glycopolymers *via* post modification methods, in particular the implementation of "click" chemistries, including thiol-ene reactions and *para*-fluoro-thiol substitution reactions [15,16]. Recently, a novel method to prepare glycopolymers, *para*-fluoro-thiol substitution of poly(pentafluorostyrene) (PPFS), has drawn considerable attention due to its simple procedure and high yields [16,17]. PPFS is prepared from pentafluorstyrene (PFS) monomer and, like other fluorinated polymers, it has many desirable properties, including low surface energy, high optical clarity, high UV, thermal, and chemical stabilities, and especially excellent antifouling properties toward lectins and other bio-agents, which could enhance the sensing specificity of the biosensors [18].

In this study we report the use of glycopolymers to fabricate PMMA polymer based LSPR optical sensor chips for the detection of concanavalin A (Con A) in a UV–Vis spectrometer. PPFS was prepared *via* a reversible addition–fragmentation chain transfer (RAFT) polymerization technique and subsequently converted into glycopolymers *via para*-fluoro-thiol "click" reactions. The prepared glycopolymers were then grafted onto the surface of PMMA sensor chips through Au–S covalent bonds. We showed the high sensitivity of these sensor chips for detection of Con A with a LOD of 1.3 nmol L^{-1} and saturated response of 1054.2 nmol L^{-1}.

2. Experimental section

2.1. Materials

A PMMA sheet of 3 mm thickness was obtained from a local commercial distributor (Shinkolite A®, original manufacturer-Mitsubishi Rayon Co., Japan) and machined into smaller pieces (9.5 mm × 25 mm). All PMMA sheets were rinsed with isopropanol and dried in a vacuum oven prior use. Ultrafine polish papers (0.3 μm aluminum oxide abrasive sheet, Thorlabs, Inc., USA) were used to remove unwanted AuNPs immobilized on the PMMA surfaces.

All reagents were obtained from Aldrich and used without further purification unless stated. *N*-(3-dimethylaminopropyl)-*N*′-ethylcarbodiimide hydrochloride (EDC, ⩾98%), *N*-hydroxysuccinimide (NHS, 98%), 2-(*N*-morpholino) ethanesulfonic acid (MES, dry powder), sodium bicarbonate (99%) and cysteamine hydrochloride (⩾97%) were used for the thiolation of PMMA substrates. Gold (III) chloride hydrate (99.999%) and sodium citrate (anhydrous, ⩾99%) were used for the preparation of AuNPs. Pentafluorostyrene (PFS, 99%) was de-inhibited by passing it through a basic alumina column prior to use. 2,2′-Azobis(2-methyl propionitrile) (AIBN, recrystallized from methanol) and 4,4′-azobis (4-cyanovaleric acid) (ABCVA, ⩾75%) were used as the initiators for the polymerization reactions. 4-Cyanopentanoic acid dithiobenzoate (CPADB, the RAFT agent) was prepared according to methods described in the literature with minor variations [19]. 1-Thio-β-D-glucose tetraacetate (97%), 1-thio-β-D-glucose sodium salt (⩾98%) and triethylamine (TEA, 99%) were used for the glycosylation of PPFS. 1-Hexylamine (99%) was used to reduce the end groups of the glycopolymers. Tris(2-carboxyethyl) phosphine hydrochloride (TCEP, 98%) was used as a thiol stabilizing agent. Concanavalin A from *Canavalia ensiformis* (Con A, Type IV, lyophilized powder) was used as the target analyte in *N*-(2-hydroxyethyl)-piperazine-*N*′-(2-ethanesulfonic acid) buffer solution (HEPES buffer solution, 99.5%). Milli-Q water (18 MΩ cm, Milli-pore, Bedford, MS) was used as a solvent and a rinsing agent.

2.2. Synthesis of AuNPs

The synthesis of AuNPs was modified slightly from techniques previously reported in the literature [20]. All glassware was cleaned with *aqua regia* solution (3:1 vol ratio of HCl and HNO_3) and then rinsed with Milli-Q water until the residual solution was completely removed (Caution!!! *aqua regia* solution is a very corrosive oxidizing agent which should be handled with great care). A solution of $HAuCl_4$ (1 mL, 1 wt%) in Milli-Q water (100 mL) was brought to boil under vigorous stirring. Sodium citrate solution (5 mL, 1 wt%) was then added rapidly into the boiling solution. The solution turned to a wine red color after prolonged boiling.

2.3. Immobilization of AuNPs on PMMA sheets

AuNPs were immobilized on the surface of thiolated PMMA sheets as shown in Scheme 1. Thiolation of native PMMA sheets were carried out by immersing the sheets in MES buffer (50 mM, pH 6) containing EDC (10 mM) and NHS (10 mM) for 3 h. Subsequently, the sheets were rinsed with Milli-Q water and immersed in carbonate buffer (50 mM, pH 9) containing cysteamine hydrochloride (50 mM) for 3 h. The resulting sheets were rinsed thoroughly with Milli-Q water and dried under nitrogen flow. The dried thiolated PMMA sheets were then immersed in a solution of AuNPs for 2 days to ensure complete particle immobilization. When the AuNP immobilization was completed, ultrafine polishing paper was used to remove AuNPs immobilized on the side and back surfaces of the PMMA sheets, leaving only the front surface immobilized with AuNPs.

2.4. RAFT polymerization of PFS using CPADB

The mixture of monomer (PFS) (6.20 mL, 44.9 mmol), RAFT agent (CPADB) (209 mg, 0.748 mmol) and initiator (ABCVA) (42.0 mg, 0.150 mmol) were dissolved in fluorobenzene (15 mL) solvent and transferred into a round bottom flask followed by air-tight sealing. The reaction mixture was degassed with nitrogen, whilst in an ice bath, for 30 min to remove oxygen. Subsequently, the round bottom flask was placed in an oil-bath, preheated to 80 °C, for 15 h. The reaction was stopped by quenching the flask in an ice bath. The resulting mixture was concentrated first under nitrogen flow and then precipitated into cold methanol to remove the residual monomer. The precipitated PPFS was washed with cold methanol and then dried in a vacuum oven for 24 h at 40 °C. Gravimetric analysis was used to determine the monomer conversion. The molecular weight and weight distribution of the resulting polymer was determined by gel permeation chromatography (GPC) and ^{1}H nuclear magnetic resonance (NMR) spectroscopy.

A series of similar polymerizations targeting different molecular weights was carried out to produce PPFS using AIBN as the initiator.

2.5. Glycosylation of PPFS

Glycosylation of PPFS was carried out by two methods described in the literatures with minor variations (Scheme S1 in Supporting Information) [16,17]. In the first method, 1-thio-β-D-glucose sodium salt was used to substitute the *para*-fluoro position in the PPFS to produce a glycopolymer [21]. PPFS (51.5 mg, 0.228 mmol PFS units, 1 eqv) and 1-thio-β-D-glucose sodium salt (79.7 mg, 0.365 mmol, 1.6 eqv) were dissolved in 4 mL anhydrous DMF. Then TEA (95.0 μL, 0.685 mmol, 3 eqv) was added to the solution. After stirring for 20 h at 35 °C, the mixture was concentrated under nitrogen flow and then precipitated into cold anhydrous ethanol. The white precipitate was filtered and washed with cold anhydrous ethanol. The resulting glycopolymer was dried in a vacuum oven for 24 h at 40 °C to yield 75.0 mg product (isolated yield = 93%).

The second method involved using 1-thio-β-D-glucose tetraacetate to substitute *para*-fluoro in the PPFS followed by deacetylation to produce glycopolymer [16]. PPFS (80.0 mg, 0.281 mmol PFS units, 1 eqv) and 1-thio-β-D-glucose tetraacetate (16.2 mg, 0.446 mmol, 1.2 eqv) were dissolved in 4 mL anhydrous DMF. Then TEA (155 μL, 1.11 mmol, 3 eqv) was added to the solution. After stirring for 20 h at 35 °C, the mixture was concentrated under nitrogen flow and then precipitated into cold anhydrous ethanol. The white precipitate was filtered and washed with cold anhydrous ethanol to afford an acetylated glycopolymer. The resulting polymer was dried in a vacuum oven for 24 h at 40 °C to yield 115 mg product (isolated yield = 64%). Then, the acetylated glycopolymer (100 mg, 0.124 mmol acetylated glucose units, 1 eqv) was dissolved in anhydrous DMF (5 mL). 0.1 M sodium methoxide in methanol (621 μL, 0.0622 mmol, 0.5 eqv) was added dropwise to the solution while rapidly stirring. After stirring for 1 h at room temperature, the reaction mixture was concentrated under nitrogen flow and then precipitated into cold anhydrous ethanol. The precipitate was further washed with cold anhydrous ethanol and fully dried in a vacuum oven for 24 h at 40 °C to give 59.1 mg final product (isolated yield = 81%).

Similar glycosylation reactions were carried out for PPFS with different molecular weights using the second method, namely the deprotection of the acetylated thioglucose unit. The conversion

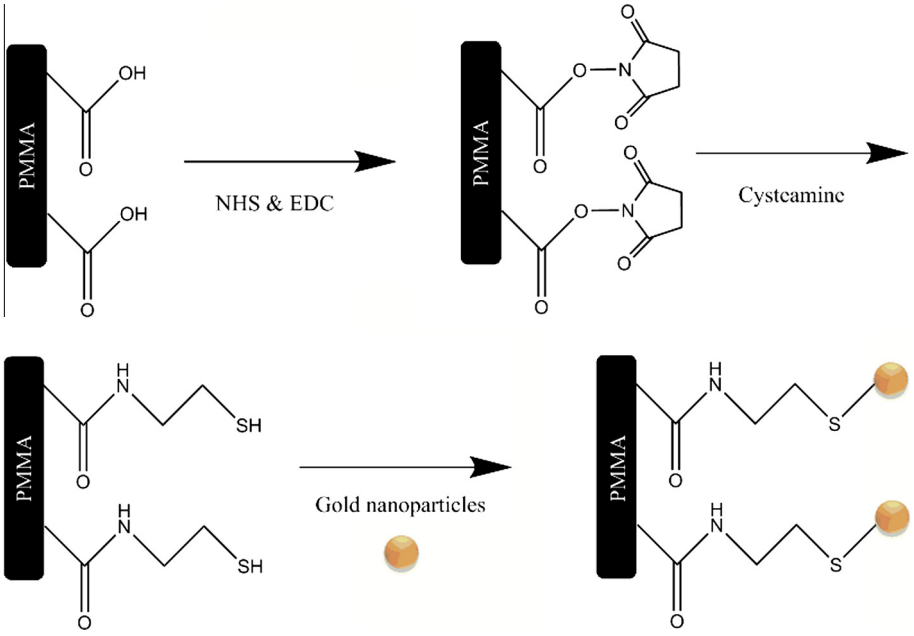

Scheme 1. Thiolation of PMMA sheets and covalent bonding of AuNPs.

and number average molecular weight of the products were determined by ^{1}H and ^{19}F NMR, respectively. The molecular weight distribution was determined by GPC.

2.6. Glycopolymer "grafted to" AuNP immobilized PMMA chips

A AuNP immobilized PMMA chip was placed into a glass vial containing 5 mL of prepared glycopolymer solution (100 μM, 5.0×10^{-7} mol, 1 eqv) followed by air-tight sealing. The solution was then purged with nitrogen for 20 min and 1.4 μL of 1-hexylamine (2.0×10^{-6} mol, 20 eqv) was added into the glass vial. A small amount of TCEP (~0.5 mg) was also added as the thiol group stabilizing agent. The reaction was carried out at room temperature in an incubator (80 rpm) for 24 h. After the reaction was completed, the glycopolymer grafted PMMA chip was thoroughly rinsed with Milli-Q water and dried in a vacuum oven for 24 h at 40 °C. The surface chemistry of the glycopolymer grafted chips was analyzed using XPS.

2.7. Con A recognition

The absorption spectra for the glycopolymer grafted PMMA sensor chips were acquired using a UV–Vis spectrophotometer. The PMMA sensor chips were fitted onto one side of a standard plastic UV–Vis cuvette with the functionalized surface facing the cuvette interior (Fig. S1 in Supporting Information).

All of the Con A binding tests were carried out in HEPES buffer solution (10 mM, pH 7.4), that contained 1 mM of Mn^{2+} and Ca^{2+}, which are essential ions for the interaction between Con A and glucose moieties [22,23]. The buffer also contained 0.1 M of NaCl to prevent aggregation of Con A at high concentrations. 2 mL of buffer solution was first added to the cuvette to record the initial plasmon band positions and then various volumes of Con A solution were added to the cuvette. All binding tests were carried out at 25 °C and the spectra were recorded 30 min after each addition, which is sufficient for complete Con A binding according to previous reports [4,24,25]. An unmodified PMMA chip in HEPES buffer was used as the background for the baseline correction. The tests were repeated with AuNP immobilized PMMA chips to determine any non-specific binding.

2.8. Characterization

2.8.1. X-ray photoelectron spectroscopy (XPS)

The surface modified PMMA chips were analyzed with an X-ray photoelectron spectrometer (ESCALAB250Xi, Thermo Scientific, UK) using a monochromated Al Kα (1486.68 eV) X-ray source with a power of 150 W. Survey and region scans were acquired at 100 eV and 20 eV, respectively. The charge neutralization was turned on during the analysis and the beam angle was set to 90°. Deconvolution of the spectral peaks was performed using the Advantage software (Thermo Scientific, UK).

2.8.2. Scanning electron microscopy (SEM)

The surface morphology of AuNP immobilized PMMA chips were observed using a field-emission scanning electron microscope (Nova NanoSEM 230, FEI, USA) at an accelerating voltage of 3 kV with a spot size of 2.5 μm. Each sample was sputter coated with chromium for 20 s at 20 mA (Emitech K575X Peltier Cooled Sputter Coater; Emitech Products Inc., USA), the coating thickness was approximately 15 nm.

2.8.3. Dynamic light scattering (DLS)

The size and ζ potential measurements of the AuNPs were performed with a Zetasizer Nano ZS (Malvern Instruments, Malvern, UK).

2.8.4. UV–Vis spectroscopy

The absorption spectra for the AuNPs and PMMA chips were acquired using a UV–Vis spectrophotometer (Cary 300 Scan, Varian, USA). Background scans were performed using water for the absorption of colloid AuNPs measurement and an unmodified PMMA chip in HEPES buffer for all sensor chip measurements. All the spectra were recorded at a resolution of 0.02 nm with at least 3 repeated measurements for each target solution.

2.8.5. Gel permeation chromatography (GPC)

Molecular weight and molecular weight distributions for all polymers were measured by GPC (Shimadzu CTO – 10A VP), using four Phenomenex columns (10.0, 10.3, 10.4, 10.6 nm pore size, 5 μm particle size) and a refractive index detector (Shimadzu RID – 10A). Dimethylacetamide (DMAc) was used as the eluent which contained 0.03 w/v% LiBr and 0.05 w/v% 3,5-di-*tert*-4-butylhydroxytoluene (BHT) stabilizer. The polymer samples were prepared at a concentration of 5 mg mL^{-1} and filtered through a 0.45 μm filter before injection, which had a flow rate of 1.0 mL min^{-1}. The column temperature was maintained at 50 °C. The system was calibrated using a series of narrow molecular weight distribution polystyrene standards from 0.5 to 1000 kDa (Polymer Laboratories). Chromatograms were analyzed using the Cirrus 3.0 software (Polymer Laboratories).

2.8.6. Nuclear magnetic resonance spectroscopy (NMR)

NMR spectra were recorded on a Bruker DPX 300 spectrometer (Bruker, Rheinstetten, Germany) at 300 MHz. All samples were dissolved in deuterated solvents with tetramethylsilane (TMS, δ 0 ppm) being used as the reference signal. NMR data was processed using the Topspin 3.2 software (Bruker).

3. Results and discussion

3.1. AuNP synthesis and surface immobilization

The AuNPs were synthesized *via* the well-known citrate reduction method [20] and characterized by DLS and UV–Vis spectroscopy. According to the DLS results, the diameter of the AuNPs was determined to be 18 nm with a PDI of 0.1. The colloidal AuNPs exhibited a sharp absorption peak at 519 nm (Fig. S2 in Supporting Information), which is in good agreement with the results reported previously for AuNPs in this size range [26–29].

After immersing the thiolated PMMA chips in colloidal AuNPs for a 2-day duration, a layer of densely packed AuNPs was observed on the substrate surface (Fig. 1A). The absorption spectrum for the AuNP immobilized PMMA chip was recorded in water medium (Fig. 1B). The spectrum exhibits a strong absorption peak at 530 nm, corresponding to the transversal LSPR band that arose when the AuNPs are isolated and devoid of interactions with neighboring particles [30]. A weak longitudinal LSPR band was also observed between 600 nm and 700 nm, which resulted from AuNP aggregates. Based on the SEM image observations as well as the resulting spectrum appearance, it can be concluded that a near monolayer of AuNPs were formed on the PMMA substrate surface with very little aggregation.

3.2. Polymerization of PFS using CPADB

The synthesized CPADB RAFT agent was determined to be greater than 90% pure by ^{1}H NMR spectroscopy (Fig. S3 in Supporting Information). Water was the main impurity remaining in the product which was difficult to remove under mild conditions due to the slight hygroscopic character of CPADB. The nature of the RAFT agent strongly affects the "livingness" of the polymerization

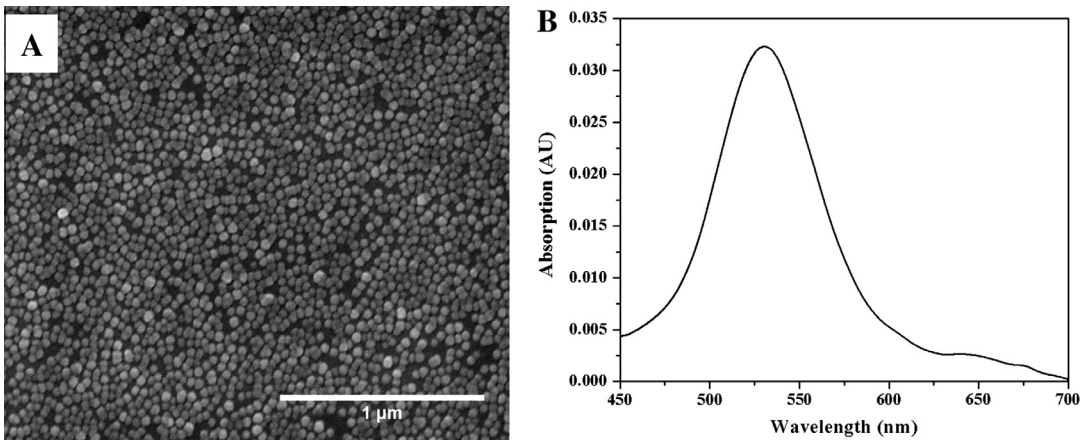

Fig. 1. SEM image of AuNPs assembled on a PMMA chip (A) and corresponding absorption spectrum in water (B).

Table 1
Characterization of the synthesized PPFS polymers.

Name	PFS/CPADB	Time (h)	Conv.[c](%)	$M_{n,theo}$ (g mol^{-1})	$M_{n,GPC}$ (g mol^{-1})	$M_{n,NMR}$ (g mol^{-1})	$Đ$	Structure
P1[a]	60	15	16.3	2200	2100	2000	1.10	$P(PFS)_{8.9}$
P2[b]	25	24	62.6	3300	3400	2800	1.12	$P(PFS)_{13.1}$
P3[b]	50	24	48.4	5000	4600	4100	1.05	$P(PFS)_{19.7}$
P4[b]	70	24	47.1	6800	5900	6600	1.08	$P(PFS)_{32.3}$

[a] ABCVA was used as the initiator.
[b] AIBN was used as the initiator.
[c] Conversions were calculated based on gravimetric analysis.

as well as the polymerization rate. It has previously been shown that CPADB has good control for the polymerization of PFS. However, the monomer conversion was found to be rather low (24%) even after 24 h when the reaction was carried out at 65 °C [31]. In order to achieve higher conversions in this study, the reaction temperature was increased to 75 °C.

Four batches of PPFS, with designated chain lengths, were prepared *via* varying the ratios between the monomer and the RAFT agent. As shown in Table 1, higher conversions of PFS were obtained except when ABCVA was used as the initiator. One possible explanation for the low conversion could be due to ABCVA's slow decomposition rate which led to an inhibition period in the initial stage of the polymerization. According to the GPC results, all polymers exhibited narrow molar mass distributions ($Đ < 1.2$). Even though the experimentally determined M_n values for PPFS were found to be close to theoretical values, PPFS exhibits a considerably different hydrodynamic volume than polystyrene in the GPC eluent (DMAc). Therefore, end group analysis was performed by comparing the integral areas of the *para* protons for the dithioester end groups to the PFS backbone protons in the ^{1}H NMR spectra to calculate the degree of polymerization and corresponding molecular weight of the polymers. The calculated polymer molecular weights based on the NMR spectra were found to be slightly lower than theoretical molecular weight, but well within experimental error.

3.3. Glycosylation of PPFS

Previous research has shown thiols to be highly reactive for the nucleophilic substitution of *para*-fluoro atoms on the PFS units in PPFS [32]. In the present study, two different strategies have been employed to obtain glycopolymers using PPFS. In the first strategy, 1-thio-β-D-glucose (1.6 eqv with respect to the PFS units) was employed to react with sample P1 which has the shortest polymer chain length among the samples prepared. ^{1}H NMR spectra of P1 and the corresponding glycopolymer generated (P1-GluOH) are shown in Fig. S4 in Supporting Information. The substituted glucose units on the polymer backbone can be confirmed by the newly emerged peaks between 6 ppm and 4 ppm. ^{19}F NMR spectra were also recorded to determine the efficiency and selectivity of the *para*-fluoro substitution reaction. As illustrated in Fig. S5 in Supporting Information, P1 exhibits three major peaks at 142.7, 153.8 and 160.8 ppm, which represent fluoro atoms at the *ortho*, *para* and *meta* positions, respectively. Upon substitution of *para*-fluoro with thioglucose, two new peaks appeared. The peak at 133.4 ppm represents the *ortho*-fluoro in the glucose substituted PFS. While the peak located at 142.2 ppm are the combination of *meta*-fluoro of the glucose substituted PFS and *ortho*-fluoro of unreacted PFS. By comparing the peak area of the *para*-fluoro atoms of the PFS units with the peak area of the *ortho*-fluoro of the glucose substituted PFS, the substitution percentage was calculated to be 73%.

Glycosylation of PPFS with thioglucose can afford the direct synthesis of glycopolymers, which was a desirable process for this study. Unfortunately, it was discovered that the substitution efficiency dropped significantly for longer PPFS chains and a large excess (>2 eqv) of thioglucose was required to achieve a sufficiently satisfactory substitution percentage for this study. A reasonable explanation was given by Chen et al. who pointed out that the strong hydrogen-bonding between free and substituted thioglucose molecules reduces the nucleophilicity of free thioglucose and resulted in a retardation effect for the substitution reaction [33]. In order to achieve higher substitution efficiencies, glycosylation of the P2, P3 and P4 samples were carried out using acetylated thioglucose (P2-GluAc, P3-GluAc, P4-GluAc respectively) followed by deprotection of the acetyl groups to afford the desired glycopolymers (P2-GluOH, P3-GluOH, P4-GluOH respectively) [16]. Although, using acetylated thioglucose requires an additional deacetylation step, it reduces the hydrogen-bonding during the *para*-fluoro substitution step. Indeed, adequate

Table 2
Characterization of the synthesized glycopolymers.

Name	Substitution (%)	$M_{n,GPC}$ (g mol^{-1})	$M_{n,NMR}$ (g mol^{-1})	$Đ$	Substituted units/polymer repeating units
P2-GluAc	77.3	8000	6400	1.19	10.1/13.1
P3-GluAc	78.5	7900	9400	1.02	15.5/19.7
P4-GluAc	68.5	10,500	14,200	1.02	22.1/32.3
P1-GluOH	73.0	10,700	3200	1.20	6.5/8.9
P2-GluOH	77.3	18,000	4600	1.19	10.1/13.1
P3-GluOH	78.5	17,600	6800	1.30	15.5/19.7
P4-GluOH	68.5	27,400	10,500	1.98	22.1/32.3

substitution percentages were obtained using less 1-thio-β-D-glucose tertraacetate (1.2 eqv with respect to PFS units) as shown in Table 2. The ^{1}H and ^{19}F NMR spectra of the corresponding acetylated glycopolymers and deacetylated glycopolymers are shown in the Supporting Information (Figs. S6–S11 in Supporting Information).

For the polymers P2, P3, and P4, substitution of *para*-fluoro atoms with acetylated thioglucose led to clear shifts of the resulting acetylated glycopolymers to higher molecular weights (Fig. 2, Tables 1 and 2). Interestingly, high molecular weight shoulders were observed for these samples which were approximately double the molecular weights of the main peaks for each sample. According to literature accounts [34], TEA added during the 'click' reactions could lead to the reduction of the dithioester RAFT agent end groups leading to thiol generation. The presence of thiol end groups could result in the formation of disulfide linkages connecting two polymer chains and thus resulting in the high molecular weight peaks. Upon deacetylation of the substituted polymers, the resulting glycopolymers' hydrodynamic volumes further increased (Fig. 2). However, adding TCEP did not lead to a significant reduction of the disulfide bonds, which can be ascribed to the interference caused by the hydrogen-bonding of the glycopolymers. Nevertheless, it has been reported that both thiols and disulfide functionalities can form covalent bonds to the gold surface [35], and a large excess of glycopolymers were used in the grafting step to offset the potential interference caused by these disulfide linkages. High molecular tails were observed in P4-GluAc and P4-GluOH, which arose from the aggregation of polymers (confirmed by DLS) due to their poor solubility in the DMAc solvent.

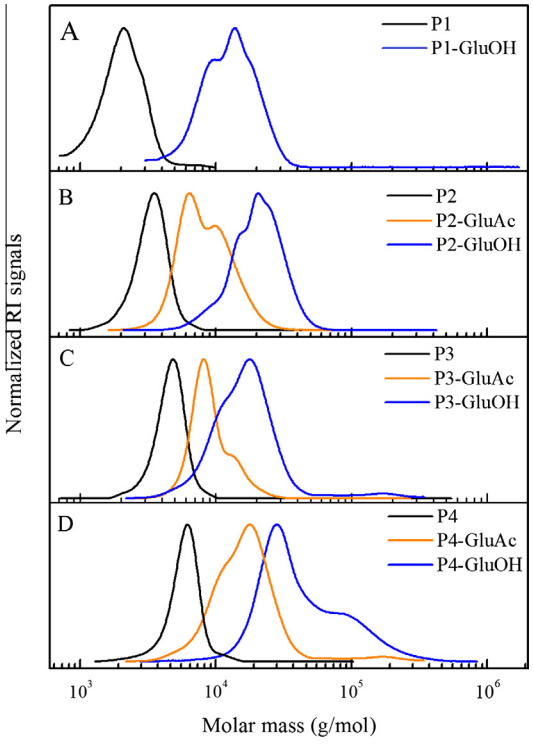

Fig. 2. Normalized GPC traces for PPFS, PPFS-GluAc and PPFS-GluOH.

3.4. Grafting glycopolymers onto the surface of sensor chips

The surfaces of the sensor chips were functionalized with glycopolymers *via* the 'grafting to' technique by reducing the dithioester end groups into thiols which can form covalent bonds with the AuNPs immobilized on the sensor surface. The concentration of the glycopolymers was 100 μM (5 mL solution, 500 nmol) which was in a large excess to the total number of Au–S bonds that can be formed on the substrate surface (1.82 nmol), assuming each Au–S bond occupies a minimum 2.17×10^{-13} mm^2 surface area [36] and the surface of the sensor chip was treated as a planar geometry with a total surface area of 238 mm^2. As this approximation from the literature was based on grafting alkanethiol compounds to gold surfaces, and our thiolated glycopolymers are considerably bulkier compounds, the existence of a large excess is a safe approximation.

XPS was used to probe the surface chemistry of the PMMA sensor chips after polymer grafting. As shown in Fig. S12A in Supporting Information, the surface survey scan of the AuNP immobilized PMMA sensor chip exhibits three apparent peaks. The C 1s emission peaks in the region between 285.0 and 289.1 eV can be assigned to the carbon from the PMMA substrate along with the O 1s peaks at 532.2 and 533.8 eV. The Au $4f_{7/2}$ emission exhibits two components: 83.82 and 84.56 eV, which represent the gold atoms in the bulk and top surface layers, respectively [37]. Trace amounts of nitrogen at ~400.3 eV (amides) and sulfur at ~161.8 eV (thiolates) were also discovered on the PMMA surface, which originated from anchored cysteamine moieties. F 1s emission was recorded at ~687.9 eV for the glycopolymer grafted PMMA substrates (Fig. S12B in Supporting Information), indicating the successful anchoring of glycopolymers onto the chip surface. Stronger nitrogen and sulfur emissions were observed in the glycopolymer grafted PMMA substrate (Fig. S12C and D in Supporting Information), which can be ascribed to the nitrogen and sulfur content in the polymer chains.

Further valuable information was obtained by analyzing the variations of the surface elemental compositions (Table 3). As can be seen, the fluorine content on the PMMA chips increases for the P1, P2, and P3 derived glycopolymers, which contain 8.9, 13.1, and 19.7 PFS units, respectively. The increase in the surface fluorine content for these samples is believed to originate from this difference in polymer chain lengths grafted to the surface rather than a higher surface grafting density. However, the fluorine content dropped slightly for the longest glycopolymer grafted to the AuNP modified PMMA surface (P4-GluOH). As the immobilization method is a 'grafting to' process, and the P4-GluOH polymer is

Table 3
Surface elemental of PMMA chips determined by XPS.

Elemental content %	AuNPs immobilized PMMA	P1-GluOH grafted PMMA	P2-GluOH grafted PMMA	P3-GluOH grafted PMMA	P4-GluOH grafted PMMA
C	69.85	66.52	65.58	66.02	66.70
O	24.90	21.68	18.85	19.8	20.66
N	0.35	0.56	1.03	0.83	0.75
F	–	4.07	7.41	7.67	6.33
S	0.17	1.38	1.97	3.10	1.72
Au	4.73	5.79	5.16	2.57	3.84

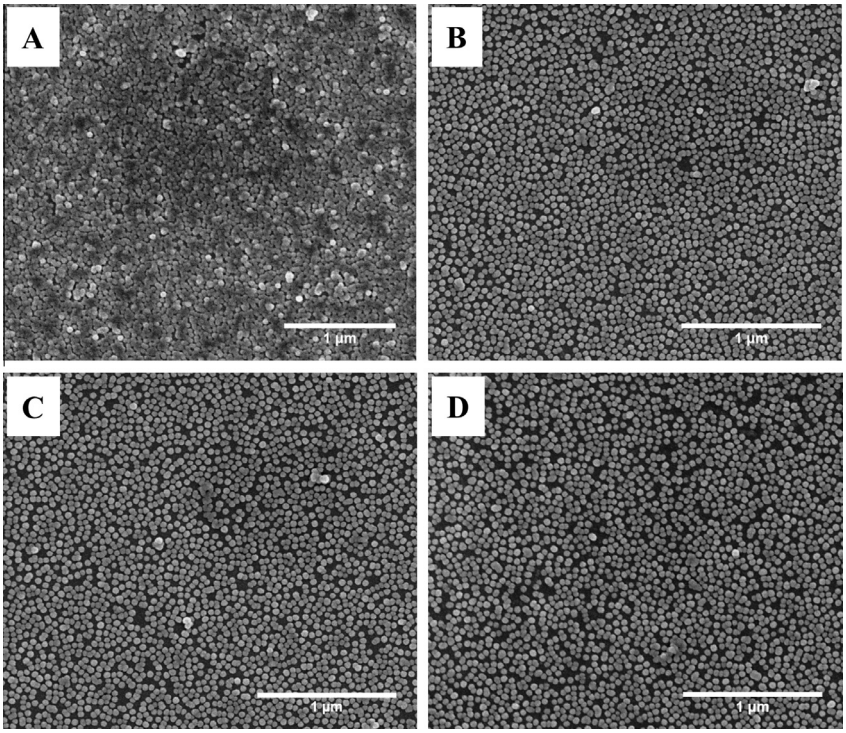

Fig. 3. SEM images of PMMA chips grafted with P1-GluOH (A), P2-GluOH (B), P3-GluOH (C), and P4-GluOH (D).

roughly 60% larger than P3-GluOH (based on degree of polymerization and molecular weight), it would follow that this fluorine content decrease stems from a slight decrease in grafting density of the polymer chains on the surface when compared to the smaller molecular weight glycopolymers. The gold composition decreased considerably after polymer grafting, which would suggest that the AuNPs on the PMMA surface are de-grafting from the surface when the larger glycopolymers were attached. The decrease in S content for the P4-GluOH grafted surface can also be ascribed to this occurrence as well, as the polymer grafting is *via* a Au–S linkage.

Inspecting the surface of the PMMA chips after polymer grafting further confirm the results obtained from the XPS studies (Fig. 3). Few AuNP aggregates/multilayers were observed on the P1-GluOH grafted surface (Fig. 3A), while the presence of these aggregates gradually diminished on the rest of the samples when grafted with longer glycopolymers. The SEM images also show that more voids among immobilized AuNPs started to appear for the samples grafted with longer glycopolymers, giving further evidence that the larger glycopolymer chains are causing the immobilized AuNPs to de-graft from the PMMA chip. Furthermore, the P1-GluOH grafted surface appeared quite different from the ones grafted with longer glycopolymers (P2-GluOH to P4-GluOH). The main reason for this difference could be ascribed to the surface density of the grafted glycopolymers. When the polymer chains are short, they can more easily diffuse into the voids between immobilized AuNPs and graft onto the side surfaces of these particles. It is believed that when the gaps between the AuNPs are narrow enough, they can be easily covered by the chromium coating required for SEM analysis. On the other hand, it would be much harder for longer glycopolymers to graft onto the side surface of AuNPs. As a result, longer glycopolymer were mostly present on the top surface of the AuNPs, and the voids between AuNPs were not reduced but enlarged due to AuNPs de-grafting events as discussed previously.

3.5. Con A recognition

Once grafted with glycopolymers, the functionalized PMMA sensor chips were tested using Con A as the target analyte. The absorption spectra for the sensor chips were obtained after a 30 min incubation with Con A at various concentrations. As shown in Fig. 4A, all of the sensor chips exhibited a red shift for the plasmon peaks. The sensor chip functionalized with the shortest glycopolymer brush (P1-GluOH) exhibited a maximum plasmon shift of 2.08 nm, while the maximum shifts gradually decreased for the sensor chips functionalized with longer glycopolymers, from 1.98 nm for P2-GluOH, to 1.46 nm for P3-GluOH, to 1.36 nm for P4-GluOH. In terms of the sensor response range, the P1-GluOH functionalized sensor chip reached a saturated response at 674.6 nmol L^{-1}. By increasing the glycopolymer length, the sat-

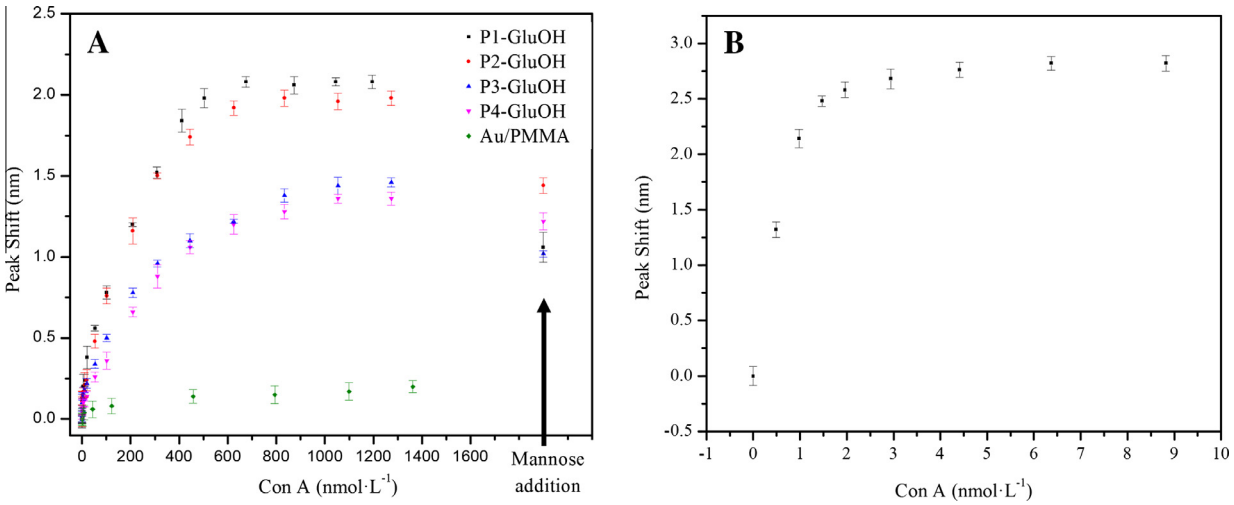

Fig. 4. Shift in plasmon bands with respect to Con A bound to glycopolymer functionalized PMMA sensor chips (A) and a 1-thio-β-D-glucose functionalized PMMA sensor chip (B).

urated response was expanded to 833.6 nmol L^{-1} for P2-GluOH and 1054.2 nmol L^{-1} for both P3-GluOH and P4-GluOH. The peak-to-peak wavelength shift noise of the sensor chips in repetitive experiments was discovered to be ~0.03 nm. Taking the LOD as 5 times this value [38], the LOD for the sensor chips can be determined to be 5.6 nmol L^{-1}, 1.3 nmol L^{-1}, 2.6 nmol L^{-1} and 20.2 nmol L^{-1} for P1-GluOH, P2-GluOH, P3-GluOH and P4-GluOH, respectively. A comparison test was carried out by functionalizing a AuNP immobilized PMMA sensor chip with 1-thio-β-D-glucose (Fig. 4B). When tested with Con A, the sensor showed a maximum shift of 2.82 nm, however the saturated response was considerably lower due to the single reactive moiety on the surface (4.4 nmol L^{-1}).

In order to confirm the responses originated from the interactions between the carbohydrate moieties on the polymer brushes and Con A, two types of control experiments were performed. To test the release of Con A from the glucose moieties, a large excess of mannose was added into the final testing solutions (to make up 10 mM). Mannose has a stronger affinity toward Con A than glucose and hence can release the surface bound Con A from the glycopolymer brushes. After 1 h incubation with mannose, all four sensor chips exhibited blue shifts, indicating the successful release of Con A from the sensor surfaces (Fig. 4A and Fig. S16 in Supporting Information). Also, it was noted that the blue shifts were less dramatic for the longer brushes, which could result from stronger multivalent interactions between the polymer chains and Con A [24]. To ensure the Con A is binding to the glycopolymer brushes, and not the latent AuNP immobilized surface, a non-functionalized AuNP sensor chip was tested (Fig. 4A). Con A solutions were introduced to the control surface and the spectral response was determined to be insignificant with a maximum shift less than 0.2 nm.

The sensing results clearly indicate that the functionalization of AuNPs with polymer brushes carrying carbohydrate moieties could greatly expand an LSPR sensor's response range by more than 200 fold. The glycopolymer brushes anchored on the sensor surface could reduce the steric hindrance for Con A binding as well as induce stronger interactions. However, the employment of glycopolymers also brought some negative impacts on the sensitivity. Although, in the comparison test, the thioglucose functionalized sensor chip showed a rather limited response range, the plasmon shifts were more dramatic than the sensor chips functionalized with glycopolymers. Furthermore, the employment of longer polymer brushes further reduced the maximum plasmon shifts when

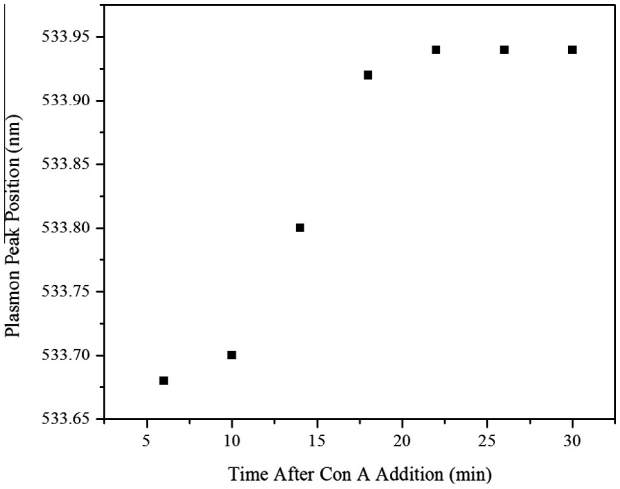

Fig. 5. Typical response time for glycopolymers functionalized PMMA sensor chip (P1-GluOH, @ 208.4 nmol L^{-1} Con A).

tested at the same concentration of analytes. This adverse effect could be explained by the location of Con A bound on the sensor surface. When the AuNPs were functionalized with thioglucose, the distance between bound Con A and AuNPs was minimized, which led to a maximum damping effect of the LSPR. On the other hand, Con A bound to polymer brushes were located further away from the AuNPs and hence led to a weaker damping effect. Furthermore, Con A bound on the tip region of the polymer brushes would bring additional steric hindrance for the subsequent binding of Con A to the interior moieties, which explains the higher LODs for longer polymer brushes. Interestingly, the P2-GluOH functionalized sensor chip showed a similar sensitivity as chips functionalized with P1-GluOH but with an even lower LOD. This could be explained by a potentially lower polymer grafting density for P2-GluOH, which provided additional space for Con A binding and offset the additional steric hindrance by Con A bound to the polymer brushes.

Due to instrument limitations, the sensor chips' real time responses were only able to be recorded in the intermediate Con A concentration ranges (200–300 nmol L^{-1}) where the shifts of the plasmon peaks were significant. A typical response curve for a sensor chip is shown in Fig. 5, with the sensor reaching full response at roughly 20 min after Con A addition, which exhibits

a similar response time when compared to results reported previously [4,25].

4. Conclusion

In conclusion, we developed a simple and efficient strategy for the fabrication of a poly(methyl methacrylate) polymer based Localized Surface Plasmon Resonance sensor chip. The preformed poly(pentafluorostyrene) was synthesized *via* a reversible addition–fragmentation chain transfer polymerization technique and subsequently converted into glycopolymers *via para*-fluoro-thiol "click" reactions. Glycopolymer brushes were successfully anchored onto the sensor surface through Au–S bonds. The testing results showed the high sensitivities of the biosensor chips for detection of concanavalin A with a limit of detection of 1.3 nmol L^{-1} and a saturated response at 1054.2 nmol L^{-1}. The influences of the length of polymer brushes on the sensor's performance were also investigated to determine the optimum length. The glycopolymer with 10–16 glucose units per chain (P2-GluOH and P3-GluOH) achieved balanced performance between sensitivities and response ranges. This research provides a general and versatile technique for developing polymer brush-grafted Localized Surface Plasmon Resonance optical sensors for the potential detection of a diverse range of analytes.

Acknowledgements

The authors thank Dr. Bill Gong at The University of New South Wales for his assistance in acquiring the XPS data, Dr. Solomon Le-Masurier and Ka Wai Fan for their assistance in the RAFT agent and polymer synthesis. The authors would also like to acknowledge the University of New South Wales (UNSW) Faculty of Engineering Early Career Researcher Faculty Research Grant (ECR/FRG) for funding of this research.

Appendix A. Supplementary material

Supplementary data associated with this article can be found in the Supporting Information. This data includes NMR, UV–Vis, and XPS plots as well as plasmon peak shifts with time for Con A release experiments. Supplementary data associated with this article can be found, in the online version, at http://dx.doi.org/10.1016/j.jcis.2015.09.047.

References

[1] K.M. Mayer, J.H. Hafner, Localized surface plasmon resonance sensors, Chem. Rev. 111 (2011) 3828–3857, http://dx.doi.org/10.1021/cr100313v.
[2] I. Abdulhalim, M. Zourob, A. Lakhtakia, Surface plasmon resonance for biosensing: a mini-review, Electromagnetics 28 (2008) 214–242, http://dx.doi.org/10.1080/02726340801921650.
[3] Y. Li, H.J. Schluesener, S. Xu, Gold nanoparticle-based biosensors, Gold Bull. 43 (2010) 29–41, http://dx.doi.org/10.1007/BF03214964.
[4] C. Guo, P. Boullanger, L. Jiang, T. Liu, Highly sensitive gold nanoparticles biosensor chips modified with a self-assembled bilayer for detection of Con A, Biosens. Bioelectron. 22 (2007) 1830–1834, http://dx.doi.org/10.1016/j.bios.2006.09.006.
[5] J. Becker, G. Reeke, B. Cunningham, G. Edelman, New evidence on the location of the saccharide-binding site of Concanavalin A, Nature 259 (1976) 406–409, http://dx.doi.org/10.1038/259406a0.
[6] W.I. Weis, K. Drickamer, Structural basis of lectin–carbohydrate recognition, Annu. Rev. Biochem. 65 (1996) 441–473, http://dx.doi.org/10.1146/annurev.bi.65.070196.002301.
[7] H. Otsuka, Y. Akiyama, Y. Nagasaki, K. Kataoka, Quantitative and reversible lectin-induced association of gold nanoparticles modified with α-lactosyl-ω-mercapto-poly(ethylene glycol), J. Am. Chem. Soc. 123 (2001) 8226–8230, http://dx.doi.org/10.1021/ja010437m.
[8] J. Wang, D. Liu, Z. Wang, Synthesis and cell-surface binding of lectin–gold nanoparticle conjugates, Anal. Methods 3 (2011) 1745–1751, http://dx.doi.org/10.1039/C1AY05151B.
[9] A. Syahir, K.-Y. Tomizaki, K. Kajikawa, H. Mihara, Poly(amidoamine)-dendrimer-modified gold surfaces for anomalous reflection of gold to detect biomolecular interactions, Langmuir 25 (2009) 3667–3674, http://dx.doi.org/10.1021/la8028275.
[10] A. Pfaff, L. Barner, A.H. Müller, A.M. Granville, Surface modification of polymeric microspheres using glycopolymers for biorecognition, Eur. Polym. J. 47 (2011) 805–815, http://dx.doi.org/10.1016/j.eurpolymj.2010.09.020.
[11] M.A. Sparks, K.W. Williams, G.M. Whitesides, Neuraminidase-resistant hemagglutination inhibitors: acrylamide copolymers containing a C-glycoside of N-acetylneuraminic acid, J. Med. Chem. 36 (1993) 778–783, http://dx.doi.org/10.1021/jm00058a016.
[12] S.S. Ting, G. Chen, M.H. Stenzel, Synthesis of glycopolymers and their multivalent recognitions with lectins, Polym. Chem. 1 (2010) 1392–1412, http://dx.doi.org/10.1039/C0PY00141D.
[13] L. Albertin, M.H. Stenzel, C. Barner-Kowollik, L.J.R. Foster, T.P. Davis, Well-defined diblock glycopolymers from RAFT polymerization in homogeneous aqueous medium, Macromolecules 38 (2005) 9075–9084, http://dx.doi.org/10.1021/ma051310a.
[14] A.M. Granville, D. Quémener, T.P. Davis, C. Barner-Kowollik, M.H. Stenzel, Chemo-enzymatic synthesis and RAFT polymerization of 6-O-methacryloyl mannose: a suitable glycopolymer for binding to the tetrameric lectin Concanavalin A?, Macromol Symp. 255 (2007) 81–89, http://dx.doi.org/10.1002/masy.200750909.
[15] L. You, H. Schlaad, An easy way to sugar-containing polymer vesicles or glycosomes, J. Am. Chem. Soc. 128 (2006) 13336–13337, http://dx.doi.org/10.1021/ja064569x.
[16] C.R. Becer, K. Babiuch, D. Pilz, S. Hornig, T. Heinze, M. Gottschaldt, U.S. Schubert, Clicking pentafluorostyrene copolymers: synthesis, nanoprecipitation, and glycosylation, Macromolecules 42 (2009) 2387–2394, http://dx.doi.org/10.1021/ma9000176.
[17] S.P. Le-Masurier, H.T.T. Duong, C. Boyer, A.M. Granville, Surface modification of polydopamine coated particles via glycopolymer brush synthesis for protein binding and FLIM testing, Polym. Chem. 6 (2015) 2504–2511, http://dx.doi.org/10.1039/C5PY00062A.
[18] M. Paz-Pazos, C. Pugh, Synthesis, isolation, and thermal behavior of polybutadiene grafted with poly(2,3,4,5,6-pentafluorostyrene), J. Polym. Sci., Part A: Polym. Chem. 43 (2005) 2874–2891, http://dx.doi.org/10.1002/pola.20765.
[19] Y. Mitsukami, M.S. Donovan, A.B. Lowe, C.L. McCormick, Water-soluble polymers. 81. Direct synthesis of hydrophilic styrenic-based homopolymers and block copolymers in aqueous solution via RAFT, Macromolecules 34 (2001) 2248–2256, http://dx.doi.org/10.1021/ma0018087.
[20] G. Frens, Controlled nucleation for the regulation of the particle size in monodisperse gold suspensions, Nature 241 (1973), http://dx.doi.org/10.1038/physci241020a0.
[21] D.H. Solomon, E. Rizzardo, P. Cacioli, Polymerization Process and Polymers Produced Thereby, U.S. Patent No. 4,581,429. 1986.
[22] Q. Yang, M.-X. Hu, Z.-W. Dai, J. Tian, Z.-K. Xu, Fabrication of glycosylated surface on polymer membrane by UV-induced graft polymerization for lectin recognition, Langmuir 22 (2006) 9345–9349, http://dx.doi.org/10.1021/la0610598.
[23] J. Yariv, A.J. Kalb, A. Levitki, The interaction of concanavalin A with methyl α-d-glucopyranoside, Biochim. Biophys. Acta, Gen. Subj. 165 (1968) 303–305, http://dx.doi.org/10.1016/0304-4165(68)90063-9.
[24] Y. Anraku, Y. Takahashi, H. Kitano, M. Hakari, Recognition of sugars on surface-bound cap-shaped gold particles modified with a polymer brush, Colloids Surf., B 57 (2007) 61–68, http://dx.doi.org/10.1016/j.colsurfb.2007.01.003.
[25] S. Morokoshi, K. Ohhori, K. Mizukami, H. Kitano, Sensing capabilities of colloidal gold modified with a self-assembled monolayer of a glucose-carrying polymer chain on a glass substrate, Langmuir 20 (2004) 8897–8902, http://dx.doi.org/10.1021/la049201x.
[26] J. Gao, X. Huang, H. Liu, F. Zan, J. Ren, Colloidal stability of gold nanoparticles modified with thiol compounds: bioconjugation and application in cancer cell imaging, Langmuir 28 (2012) 4464–4471, http://dx.doi.org/10.1021/la204289k.
[27] S.M. Agnihotri, H. Ohshima, H. Terada, K. Tomoda, K. Makino, Electrophoretic mobility of colloidal gold particles in electrolyte solutions, Langmuir 25 (2009) 4804–4807, http://dx.doi.org/10.1021/la803671t.
[28] A. Mocanu, I. Cernica, G. Tomoaia, L.-D. Bobos, O. Horovitz, M. Tomoaia-Cotisel, Self-assembly characteristics of gold nanoparticles in the presence of cysteine, Colloids Surf., A 338 (2009) 93–101, http://dx.doi.org/10.1016/j.colsurfa.2008.12.041.
[29] H.M. Zakaria, A. Shah, M. Konieczny, J.A. Hoffmann, A.J. Nijdam, M.E. Reeves, Small molecule-and amino acid-induced aggregation of gold nanoparticles, Langmuir 29 (2013) 7661–7673, http://dx.doi.org/10.1021/la400582v.
[30] J. Schmitt, P. Mächtle, D. Eck, H. Möhwald, C.A. Helm, Preparation and optical properties of colloidal gold monolayers, Langmuir 15 (1999) 3256–3266, http://dx.doi.org/10.1021/la981078k.
[31] N.t. Brummelhuis, M. Weck, RAFT polymerization of alternating styrene–pentafluorostyrene copolymers, J. Polym. Sci., Part A: Polym. Chem. 52 (2014) 1555–1559, http://dx.doi.org/10.1002/pola.27148.
[32] D. Samaroo, M. Vinodu, X. Chen, C.M. Drain, Meso-Tetra (pentafluorophenyl) porphyrin as an efficient platform for combinatorial synthesis and the selection of new photodynamic therapeutics using a cancer cell line, J. Comb. Chem. 9 (2007) 998–1011, http://dx.doi.org/10.1021/cc070067j.

[33] J. Chen, L. Dumas, J. Duchet-Rumeau, E. Fleury, A. Charlot, D. Portinha, Tuning h-bond capability of hydroxylated-poly(2,3,4,5,6-pentafluorostyrene) grafted copolymers prepared by chemoselective and versatile thiol-para-fluoro "click-type" coupling with mercaptoalcohols, J. Polym. Sci., Part A: Polym. Chem. 50 (2012) 3452–3460, http://dx.doi.org/10.1002/pola.26136.
[34] P.J. Roth, C. Boyer, A.B. Lowe, T.P. Davis, RAFT polymerization and thiol chemistry: a complementary pairing for implementing modern macromolecular design, Macromol. Rapid Commun. 32 (2011) 1123–1143, http://dx.doi.org/10.1002/marc.201100127.
[35] J.C. Love, L.A. Estroff, J.K. Kriebel, R.G. Nuzzo, G.M. Whitesides, Self-assembled monolayers of thiolates on metals as a form of nanotechnology, Chem. Rev. 105 (2005) 1103–1170, http://dx.doi.org/10.1021/cr0300789.
[36] C. Vericat, M. Vela, R. Salvarezza, Self-assembled monolayers of alkanethiols on Au (111): surface structures, defects and dynamics, Phys. Chem. Chem. Phys. 7 (2005) 3258–3268, http://dx.doi.org/10.1039/B505903H.
[37] K. Heister, M. Zharnikov, M. Grunze, L. Johansson, Adsorption of alkanethiols and biphenylthiols on Au and Ag substrates: a high-resolution X-ray photoelectron spectroscopy study, J. Phys. Chem. B 105 (2001) 4058–4061, http://dx.doi.org/10.1021/jp010127q.
[38] A.J. Haes, L. Chang, W.L. Klein, R.P. Van Duyne, Detection of a biomarker for Alzheimer's disease from synthetic and clinical samples using a nanoscale optical biosensor, J. Am. Chem. Soc. 127 (2005) 2264–2271, http://dx.doi.org/10.1021/ja044087q.